PNAS RESEARCH ARTICLE | APPLIED BIOLOGICAL SCIENCES OPEN ACCESS

Synergistic action of different molecular mechanisms causes striking levels of insecticide resistance in the malaria vector *Anopheles gambiae*

Mengling Chen[a,b], Latifa Remadi[b], Dimitra Tsakireli[b], Emmanouil Kokkas[a,b], Sofia Balaska[b], Sibora Teta[a,b], Jocelyn M. F. Ooi[c], Janet Hemingway[c,1], Mark J. I. Paine[c], Gareth J. Lycett[c], John Vontas[b,d,1], and Linda Grigoraki[b,1]

Affiliations are included on p. 10.

Contributed by Janet Hemingway; received February 13, 2026; accepted June 8, 2026; reviewed by Lyric Bartholomay, Lizette L. Koekemoer, Charles Robin, and Daniel Swale

Intensifying insecticide resistance in the malaria vector *Anopheles gambiae* poses a serious threat to the progress achieved the last decades in reducing malaria deaths in Africa. The genetic basis of insecticide resistance is often complex, involving multiple genes and mutations. However, we still lack a clear understanding of how each mechanism contributes to overall resistance and how highly resistant phenotypes arise. In this study, we generated a suite of transgenic *An. gambiae* strains carrying either individual mechanisms or combinations that frequently co-occur in nature. We show that co-overexpression of different detoxification enzymes (CYP6P3, CYP6M2, CYP9K1, ABCH2, GSTE2, and COEAE6G), as well as the overexpression of detoxification enzymes in the presence of target site resistance mutations, can lead to substantially greater levels of resistance. Our findings suggest that increased resistance strength is a primary driver for selection of multimechanism resistance and are transformative for the scientific insight required to design robust molecular diagnostics for timely and reliable resistance detection in the field. We further show that P450 based resistance can constitute an Achilles heel for highly resistant mosquitoes, making them more vulnerable to proinsecticides; compounds that typically require P450 activation. Our results advance our understanding of the mechanistic basis of insecticide resistance and have important implications for the design and implementation of effective and evidence-based resistance management strategies.

malaria | functional genetics | resistance mechanisms | synergism | resistance management

Significance

Managing the increasing problem of insecticide resistance in malaria vectors requires a detailed understanding of its genetic basis. Although several genes have been associated with resistance, little is known about their complex interactions and how these shape phenotypic outcomes. Here, we provide functional evidence that combinations of resistance mechanisms, including the overexpression of different detoxification enzymes and the coexistence of metabolic and target site resistance, can act synergistically, leading to multiplicatively stronger resistance phenotypes. These interactions are critical for accurate diagnosis of resistance. Furthermore, we highlight the importance of assessing in vivo whether P450s predominantly activate or detoxify proinsecticides, as this can tip the balance toward cross or negative cross-resistance, with important implications for their deployment in resistance management.

Malaria remains a major cause of mortality and morbidity in Africa, with close to 610,000 deaths reported in 2024 (1). Implementation of vector control tools reliant on insecticides, including insecticide-treated bed nets (ITNs) and indoor residual spraying (IRS), has largely contributed in reducing the disease incidence (2), but their power and sustainability are threatened by the selection of high levels of insecticide resistance (3, 4).

In the last decade, a wealth of studies has identified and characterized genes in the main malaria vector *Anopheles gambiae* with a role in insecticide resistance using transcriptomic, genomic, and molecular approaches (5–7). Two main categories of resistance mechanisms have been described: the toxicokinetic, that involve mutations at the insecticide target sites that reduce binding efficiency, and the toxicodynamic, that reduce the amount of insecticide reaching its target, either through increased metabolism and sequestration or decreased penetration and increased excretion (8).

Among the most well-known toxicokinetic cases are mutations in the pyrethroid target site, the voltage gated sodium channel (VGSC), with the classical L995F (widely known as L1014F) mutation being widespread in field populations, often reaching fixation (9). This mutation has been previously functionally validated through CRISPR editing showing to confer up to 14-fold resistance to pyrethroids (10).

In the case of toxicodynamic mechanisms, cytochrome P450s have been characterized as a key enzyme family involved in detoxification of xenobiotics through hydroxylation (Phase I metabolism) (11, 12). In *Anopheles gambiae* mosquitoes, overexpression of members of the CYP6 and CYP9 families, including *Cyp6m2*, *Cyp6p3,* and *Cyp9k1* are commonly overexpressed in resistant populations and have been shown to metabolize pyrethroids (12–14). Glutathione *S*-transferases have also been associated with insecticide resistance. They can act either directly by adding a glutathione molecule to their substrate insecticide, rendering it more water soluble (Phase II metabolism) or indirectly through sequestration and/or reduction of oxidative stress (15). *Gste2* has been shown to confer

The authors declare no competing interest.

[1]To whom correspondence may be addressed. Email: janet.hemingway@lstmed.ac.uk, vontas@imbb.forth.gr, or linda_grigoraki@imbb.forth.gr.

This article contains supporting information online at https://www.pnas.org/lookup/suppl/doi:10.1073/pnas.2604812123/-/DCSupplemental.

Published July 20, 2026.

resistance to DDT and fenitrothion in *An. gambiae*, while it has also been associated with resistance to permethrin (16, 17). Carboxyl-esterases are another type of detoxification enzyme that act primarily through sequestration of their substrate. Recently *Coeae6g* was functionally validated showing to confer resistance to the organophosphate pirimiphos-methyl and permethrin (18). Increased excretion of insecticides has also been described as a resistance mechanism (Phase III), but is less well characterized. Evidence was provided previously for the association of the ABCH2 transporter in deltamethrin toxicity, by acting as a pyrethroid exporter located in the legs (19).

Although there are cases in mosquitoes where a single mechanism has been described to drive resistance, as is the case of mutations in the chitin synthase in *Culex pipiens,* conferring high levels of resistance to diflubenzuron (20) and the overexpression of *Cyp6P9a/b* in *An. funestus* conferring pyrethroid resistance (21), in most cases resistance has a complex genetic basis where multiple genes are associated with the phenotype (12, 22–24). *An. gambiae* field populations frequently harbor target site resistance mutations alongside the overexpression of various detoxification enzymes, from the same and/or different enzyme families (25). In those more complex cases it is important to understand how different mechanisms combine to shape resistance levels. Are individual mechanisms sufficient to confer resistance and to what extent? Moreover, does the coexistence of different mechanisms result in additive or even synergistic effects that would explain their persistence in the same genetic background? Gaining this knowledge is essential for understanding the dynamics of insecticide resistance evolution and designing efficient resistance surveillance and management strategies.

In this study, we used a large panel of transgenic strains and crosses between them to validate the role of multiple detoxification enzymes, including the P450s CYP6P3, CYP6M2, CYP9K1; the carboxyl esterase COEAE6G; the glutathione S-transferase GSTE2 and the ABC transporter ABCH2, when alone or in combination with each other or the *kdr* target site mutation, in conferring pyrethroid resistance and its magnitude. We also used the P450 overexpressing strains to study the phenotypic responses to proinsecticide exposure. Proinsecticides require activation to their more toxic form by endogenous P450s, and thus are considered a good option for managing resistant populations with elevated P450 expression. However, as P450s can also detoxify proinsecticides, it is critical to know if their activation or detoxification will prevail in vivo, especially in cases where in vitro metabolism assays provide inconclusive results (26). Here, we test cross resistance to the mitochondrial uncoupler chlorfenapyr, a new generation malaria preventative product that is used in dual insecticide bednets, the sodium channel blocker indoxacarb and the organophosphate pirimiphos-methyl, that is increasingly being used in IRS applications (27, 28).

Results

Functional Validation of Resistance Levels Conferred by the Overexpression of Abch2 Alone and in Combination with Cyp6p3. We used the GAL4-UAS system to overexpress *Abch2* in a susceptible lab strain and validate its role in resistance functionally. Initially a UAS-Abch2 responder line marked with YFP (under the 3× P3 promoter) was generated through site-directed recombination-mediated cassette exchange (RMCE) into the CFP marked (under the 3× P3 promoter) A11 docking line [2× attP, generated in Adolfi et al. (14)] (*SI Appendix*, Fig. S1*A*). Seven F1 progeny were identified with cassette exchange (marked with YFP only) and used for the establishment of the line (details provided in *SI Appendix*, Table S2). The UAS-Abch2 line was crossed to a GAL4 driver line that expresses the trans-activator under the ubiquitin promoter (Ubi-GAL4), driving expression in multiple tissues [line generated and described in Adolfi et al. (14, 29)]. Progeny of this cross transcribed *Abch2* (hereafter marked Abch2$^+$) at approximately 66-fold (*SI Appendix*, Fig. S2*A*) higher levels compared to the A11 parental line.

To assess how the *Abch2* overexpression impacts the susceptibility of mosquitoes to insecticides, we used female Abch2$^+$ and exposed them to WHO tube susceptibility bioassays. WHO tube assays are used to assess the presence of resistance by exposing mosquitoes to discriminating doses (twice the lethal concentration that kills 99% of a susceptible population). Mortality (24 h post exposure) of less than 90% indicates resistance (30). Of seven insecticides tested (the pyrethroids: deltamethrin, permethrin, and α-cypermethrin; the organophosphates: malathion and pirimiphos-methyl, the carbamate: bendiocarb, and the organochlorine: DDT), no resistance was observed for Abch2$^+$ mosquitoes (100% mortality, 24 h post exposure) (*SI Appendix*, Fig. S3*A*). However, a significantly lower knock down rate (defined as the inability to stand up within an hour of exposure) compared to the control A11 group was observed for the three pyrethroids (*SI Appendix*, Fig. S3*B*).

To investigate further whether *Abch2* provides reduced susceptibility to pyrethroids, we used WHO papers impregnated with 0.016% deltamethrin, instead of the 0.05% discriminating dose, as previously used by Kefi et al. (19). We also varied the exposure time, to estimate the Lethal time 50 (LT_{50}) and quantify susceptibility levels. Significantly lower mortality was observed for Abch2$^+$ mosquitoes compared to control mosquitoes at all time points tested, except for the 90 min when both strains reached approximately 100% mortality (Fig. 1*A*). The LT_{50} of the Abch2$^+$ was estimated at 25 min. Given that at 3 min exposure, mortality of the A11 was around 50%, the *Abch2* overexpressing mosquitoes show a minimum resistance ratio of eightfold at the 0.016% deltamethrin dose (Fig. 1*A* and *SI Appendix*, Table S1).

To assess whether there is a combined effect of ABCH2 and P450 overexpression, we co-overexpressed the transporter with *Cyp6p3*. To do so, we initially generated a line combining at the same locus the Ubi-GAL4 and the UAS-Cyp6p3 elements, thus natively overexpressing *Cyp6p3,* without the need of crossing. To generate this line, we used the Ubi-GAL4 line as a docking line and integrated the UAS-Cyp6p3 cassette (individuals marked YFP and CFP), as depicted in *SI Appendix*, Fig. S4*A* and described by Adolfi et al. (14). The generated Ubi-GAL4: UAS-Cyp6p3 line (in short hereafter GAL4-Cyp6p3$^+$) natively overexpressed *Cyp6p3* at 401-fold (transgene at one copy), which is lower than the 573-fold overexpression of *Cyp6p3* seen in progeny of the Ubi-GAL4 x UAS-Cyp6p3 (strain previously generated by Adolfi et al. 14) cross, but shows similar resistance levels (*SI Appendix*, Fig. S4 *B–D*). The GAL4-Cyp6p3$^+$ strain was crossed to the UAS-Abch2 and progeny (Abch2$^+$+Cyp6p3$^+$) (*SI Appendix*, Fig. S1*B*) were tested for the overexpression of both genes (122-fold for *Cyp6p3* and 21-fold for *Abch2*) (*SI Appendix*, Fig. S2*D*).

Abch2$^+$+Cyp6p3$^+$ mosquitoes showed significantly lower mortality to the 1× diagnostic dose of deltamethrin and permethrin compared to mosquitoes overexpressing only one of the two genes (Fig. 1 *C* and *D*). To assess the strength of resistance, exposure to 5× and 10× diagnostic doses is recommended by WHO. Abch2$^+$+Cyp6p3$^+$ mosquitoes showed 100% mortality at the 5× diagnostic dose (Fig. 1 *C* and *D*).

Functional Validation of Resistance Levels Conferred by the Overexpression of Cyp9k1 Alone and in Combination with Cyp6p3. A UAS-Cyp9k1 responder line, marked with YFP (under

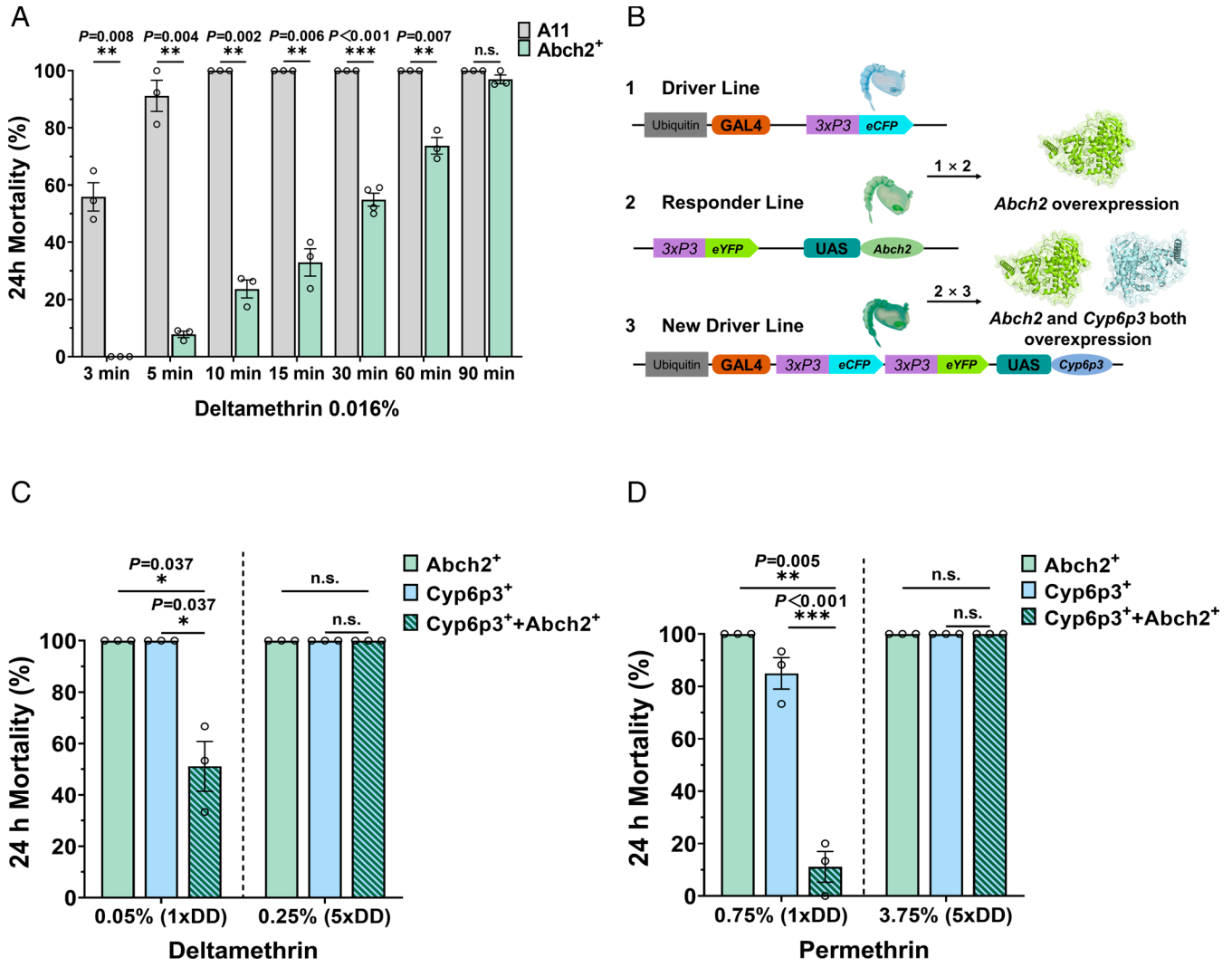

Fig. 1. Evaluating the effect of multitissue overexpression of *Abch2*, when alone and in combination with *Cyp6p3* on pyrethroid susceptibility. (*A*) Percentage mortality of Abch2$^+$ and control (A11) mosquitoes 24 h after exposure to 0.016% deltamethrin impregnated papers in a WHO tube assay across different exposure times. (*B*) Schematic diagram showing the Ubi-GAL4 driver (numbered 1), the UAS-Abch2 responder (numbered 2), and the Ubi-GAL4: UAS-Cyp6p3 (numbered 3) line, as well as how the GAL4/UAS system drives overexpression of the target genes either individually (crossing 1 with 2) or in combination (crossing 2 with 3). (*C*) Percentage mortality of mosquitoes overexpressing *Abch2* (Abch2$^+$), *Cyp6p3* (Cyp6p3$^+$) or their combination (Abch2$^+$+Cyp6p3$^+$), 24 h after exposure to 1× (0.05%) and 5× (0.25%) WHO diagnostic dose of deltamethrin. (*D*) Percentage mortality of Abch2$^+$, Cyp6p3$^+$ and Abch2$^+$+ Cyp6p3$^+$ mosquitoes, 24 h after exposure to 1× (0.75%) and 5× (3.75%) WHO diagnostic dose of permethrin. For all bioassays, at least three biological replicates were performed, each comprising 20 to 25 3 ~ 5-day-old females. Individual data points represent different biological replicates, and bars indicate the SE. Statistical significance was assessed using Welch's *t* test (n.s., not significant, *P < 0.05, **P < 0.01; ***P < 0.001).

the 3× P3 promoter) was generated as described in the previous section for the UAS-Abch2 strain. Details of the establishment of the strain are provided in *SI Appendix*, Fig. S1*B* and Table S2. Progeny of the cross between UAS-Cyp9k1 and the driver line Ubi-GAL4 (in short Cyp9k1$^+$) overexpressed *Cyp9k1* 19-fold (*SI Appendix*, Fig. S2*B*).

Mosquitoes overexpressing *Cyp9k1* were exposed to WHO discriminating doses of several insecticides. Resistance was observed for the pyrethroids: deltamethrin (67% mortality), permethrin (19% mortality), and α-cypermethrin (18% mortality) (Fig. 2). A smaller, but significant reduction in mortality to DDT (85%) was also observed. No resistance was observed for bendiocarb, malathion, and pirimiphos-methyl (Fig. 2). We produced time response curves to quantify LT_{50} resistance levels of Cyp9k1$^+$ mosquitoes. The resistance ratio was estimated at ≥12-fold for deltamethrin, 11-fold for permethrin, ≥29-fold for α-cypermethrin and twofold for DDT (Table 1).

Next, we assessed whether there is a combined effect between *Cyp9k1 and Cyp6p3* overexpression. We crossed the GAL4-Cyp6p3$^+$ strain with the UAS-Cyp9k1 responder line and measured the overexpression levels of both genes in their progeny (Cyp9k1$^+$+Cyp6p3$^+$): 26-fold for *Cyp9k1* and 125-fold for *Cyp6p3* (*SI Appendix*, Fig. S2*E*). Resistance, and its strength to deltamethrin and permethrin were evaluated through WHO tube bioassays using 1×, 5× and 10× diagnostic doses. Mosquitoes overexpressing both P450s showed resistance not only to the 1× deltamethrin and 1× permethrin, but also to the 5× deltamethrin and 5× permethrin diagnostic dose with significantly lower mortality compared to mosquitoes overexpressing only one of the two genes (Fig. 3 *A* and *B*). 100% mortality was observed in the 10× diagnostic doses for all strains (Fig. 3 *A* and *B*).

To test if the observed effect is due to higher expression of pyrethroid metabolizing P450s or higher expression of the specific two P450s, we crossed the GAL4-Cyp6p3$^+$ strain to the responder

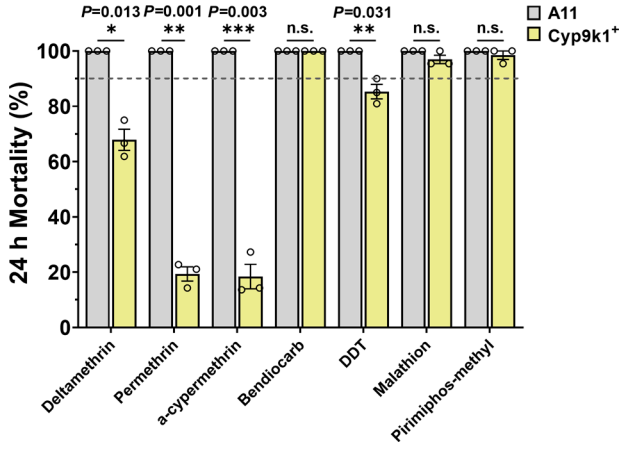

Fig. 2. WHO susceptibility bioassays for testing the effect of multitissue *Cyp9k1* overexpression on insecticide resistance. Percentage mortality of *Cyp9k1* overexpressing (Cyp9k1$^+$) and control (A11) mosquitoes 24 h after 1 h exposure to the 1× WHO diagnostic dose of different insecticides (0.05% deltamethrin, 0.75% permethrin, 0.05% α-cypermethrin, 0.1% bendiocarb, 4% DDT, 5% malathion, and 0.25% pirimiphos-methyl). For all bioassays, at least three biological replicates were performed, each comprising 20 to 25 randomly selected 3 ~ 5-day-old females. Individual data points represent different biological replicates, and bars indicate the SE. The dotted line indicates the WHO 90% mortality threshold used to define resistance. Statistical significance was assessed using Welch's *t* test (n.s., not significant, **P* < 0.05, ***P* < 0.01; ****P* < 0.001).

line UAS-Cyp6p3 and assessed pyrethroid resistance of their progeny (Cyp6p3$^+$+Cyp6p3$^+$). Progeny showed 898-fold overexpression of *Cyp6p3* (*SI Appendix*, Fig. S4*B*), and low or no resistance to the 1×, 5×, and 10× diagnostic dose of deltamethrin and permethrin (*SI Appendix*, Fig. S4 *C* and *D*).

Evaluating the Combined Effect of Two Different Types of Detoxification Enzymes. We next tested the combined effect of two enzymes belonging to different detoxification enzyme families. We combined the overexpression of *Cyp6p3* with that of *Gste2* and of the carboxylesterase *Coeae6g*. To do that we crossed the GAL4-Cyp6p3$^+$ strain with previously generated UAS-Gste2 and UAS-Coeae6g responder lines (14, 18). From those crosses, we obtained progeny overexpressing *Cyp6p3* and *Gste2* (Cyp6p3$^+$+Gste2$^+$) and progeny overexpressing *Cyp6p3* and *Coeae6g* (Cyp6p3$^+$+Coeae6g$^+$) (*SI Appendix*, Fig. S2 *F* and *G*), respectively. We also crossed Ubi-GAL4 separately with the UAS-Cyp6p3, UAS-Gste2, and UAS-Coeae6g lines to obtain progeny that overexpress only one gene. Cyp6p3$^+$+Gste2$^+$ mosquitoes were susceptible to deltamethrin, having the same response as the Cyp6p3$^+$ and Gste2$^+$ mosquitoes (Fig. 4*A*), while for permethrin they showed a small but significant decrease in mortality compared to Cyp6p3$^+$ and Gste2$^+$ mosquitoes in the 1× diagnostic dose. The Cyp6p3$^+$+Coeae6g$^+$ progeny were tested for permethrin and pirimiphos-methyl, two insecticides that have been shown to interact in vitro with both CYP6P3 and COEAE6G (18, 26). The Cyp6p3$^+$+Coeae6g$^+$ mosquitoes showed significantly lower mortality compared to the strains expressing one of the two enzymes when exposed to 1× and 5× diagnostic doses of permethrin (Fig. 4*C*), while for pirimiphos-methyl they had the same response as the Coeae6g$^+$ mosquitoes (Fig. 4*D*) (18).

Table 1. Time-response toxicity assays for estimating resistance strength of *Cyp9k1* overexpressing mosquitoes

Line	Insecticides	LT_{50}	95% FL	Slope ± SE	RR
A11	Deltamethrin	<3			
	Permethrin	7.3*			
	α-Cypermethrin	<3			
	DDT	19.74	17.56 – 22.25	3.63 ± 0.36	
Cyp9k1$^+$	Deltamethrin	38.06	32.71 – 43.56	3.10 ± 0.31	>12.67
	Permethrin	81.46	69.89 – 93.98	4.34 ± 0.41	11.16
	α-Cypermethrin	89.82	79.12 – 101.83	4.49 ± 0.56	>29.94
	DDT	47.06	43.09 – 51.43	8.94 ± 0.80	2.39

Cyp9k1$^+$ and A11 control mosquitoes were exposed to the 1× diagnostic dose of insecticides in WHO tube assays varying the exposure time. The LT_{50} (time in min required to obtain 50% mortality) is provided for each strain with the 95% fiducial limits (95% FL) and was used for calculating the resistance ratio (RR) (LT_{50} of Cyp9k1$^+$/LT_{50} of A11). Each bioassay included at least five exposure time points. For each time point three replicates were included, of 20 to 25, 3 ~ 5-day-old female mosquitoes. *A11's LT_{50} value for permethrin was obtained from a previous publication using the same strain (18).

Evaluating the Combined Effect of Target Site and Metabolic Resistance. We also tested the combined effect of metabolic and target site resistance mechanisms by combining the VGSC mutation L995F (hereafter called *kdr*) with the overexpression of *Cyp6p3* and *Cyp6m2*. We introduced the *kdr* mutation in the driver (Ubi-GAL4) and responder lines (UAS-Cyp6p3 and UAS-Cyp6m2) through crosses with a previously generated CRISPR edited line, that carries the 995F mutation in an insecticide susceptible genetic background (10). More details on the establishment of the Ubi-GAL4+*kdr*, UAS-Cyp6p3+*kdr,* and UAS-Cyp6m2+*kdr* lines and crosses performed are provided in *SI Appendix*, Fig. S5 *A–E*.

The combination of *kdr* with overexpression of *Cyp6p3* conferred high levels of resistance to deltamethrin in all: 1×, 5×, and 10× diagnostic doses compared to the strains carrying only one of the two mechanisms (Fig. 5*A*). The combination of *kdr* mutation

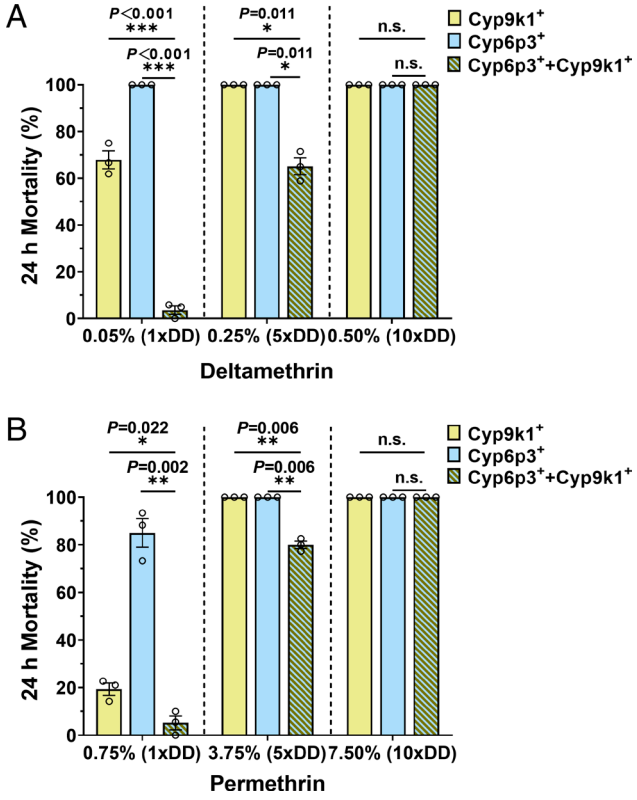

Fig. 3. Evaluating the effect of *Cyp9k1* and *Cyp6p3* co-overexpression on pyrethroid resistance levels. (*A*) Percentage mortality of mosquitoes overexpressing *Cyp9k1* (Cyp9k1$^+$), *Cyp6p3* (Cyp6p3$^+$), or their combination (Cyp9k1$^+$+Cyp6p3$^+$) 24 h after 1 h exposure to the 1× (0.05%), 5× (0.25%) and 10× (0.50%) WHO diagnostic dose of deltamethrin. (*B*) Percentage mortality of Cyp9k1$^+$, Cyp6p3$^+$, and Cyp9k1$^+$+Cyp6p3$^+$ mosquitoes 24 h after exposure to the 1× (0.75%), 5× (3.75%) and 10× (7.50%) WHO diagnostic dose of permethrin. For all bioassays, at least three replicates were performed, each comprising 20 to 25, 3 ~ 5-day-old females. Individual data points represent different replicates, and bars indicate the SE. Statistical significance was assessed using Welch's *t* test (n.s., not significant, **P* < 0.05, ***P* < 0.01; ****P* < 0.001).

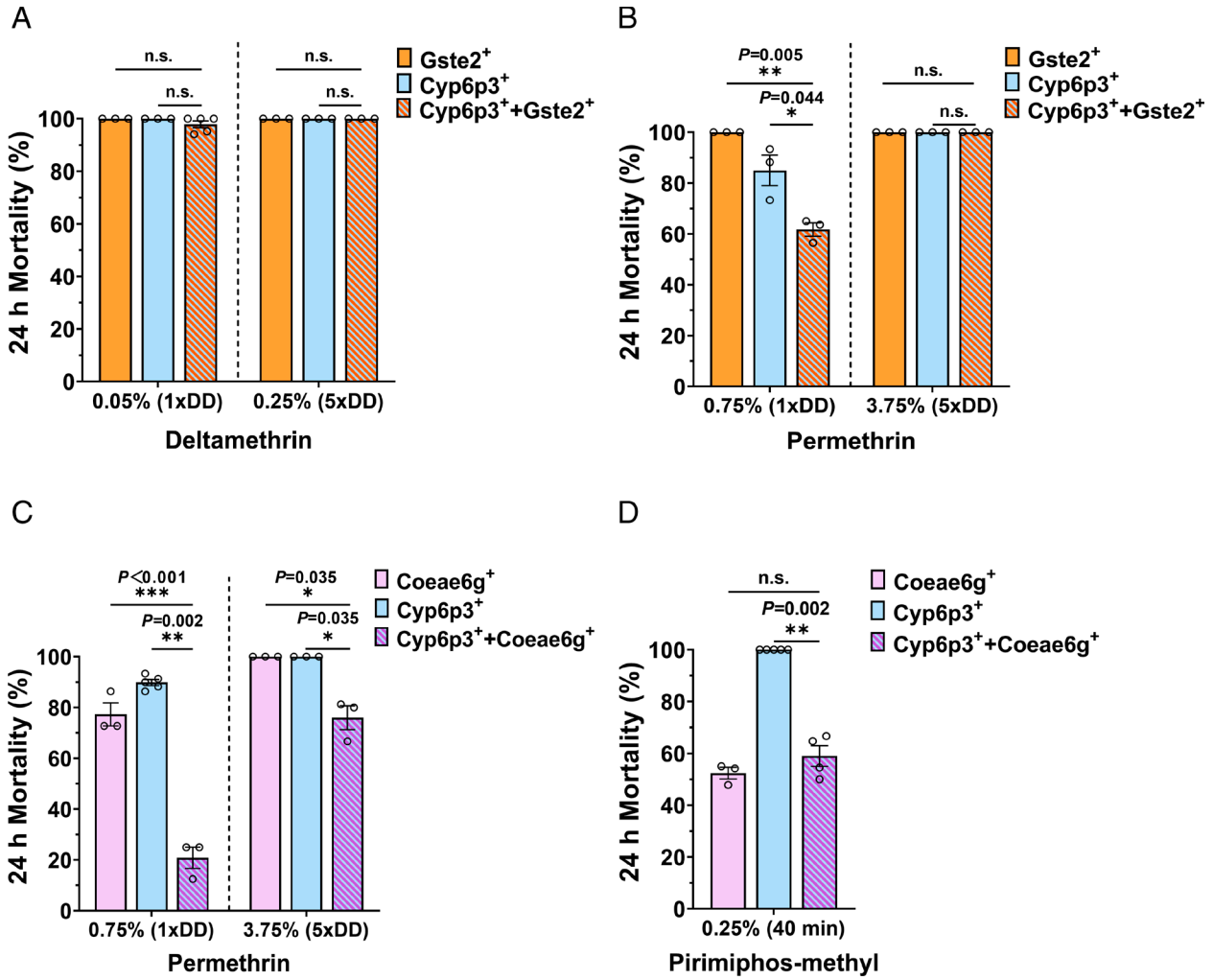

Fig. 4. Evaluating the effect of *Cyp6p3* co-overexpression with *Gste2* or *Coeae6g* on insecticide resistance levels. (*A*) Percentage mortality of mosquitoes overexpressing *Gste2* (Gste2$^+$), *Cyp6p3* (Cyp6p3$^+$), or their combination (Gste2$^+$+Cyp6p3$^+$) 24 h after 1 h exposure to the 1× (0.05%) and 5× (0.25%) WHO diagnostic dose of deltamethrin and (*B*) 1 h exposure to the 1× (0.75%) and 5× (3.75%) WHO diagnostic dose of permethrin. (*C*) Percentage mortality of mosquitoes overexpressing *Coeae6g* (Coeae6g$^+$), *Cyp6p3* (Cyp6p3$^+$), or their combination (Coeae6g$^+$+Cyp6p3$^+$) 24 h after 1 h exposure to the 1× (0.75%) and 5× (3.75%) WHO diagnostic dose of permethrin and (*D*) 40 min exposure the 1× (0.25%) diagnostic dose of pirimiphos-methyl, which is the previously estimated LT_{50} for Coeae6g$^+$. For all bioassays, at least three replicates were performed, each comprising 20 to 25, 3 ~ 5-day-old females. Individual data points represent different replicates, and bars indicate the SE. Statistical significance was assessed using Welch's *t* test (n.s., not significant, **P* < 0.05, ***P* < 0.01; ****P* < 0.001).

with the overexpression of *Cyp6m2,* conferred resistance and significantly lower mortality compared to the strains carrying one of the two mechanisms, only in the case of the 1× diagnostic dose (Fig. 5*B*). We also generated time response curves to deltamethrin and estimated the LT_{50} values for all strains (Table 2). As shown in Table 2, the LT_{50} values for the Cyp6p3$^+$+*kdr* and Cyp6m2$^+$+*kdr* strains are greater than the sum of the LT_{50} values of the individual mechanisms. Thus, the combination of the two mechanisms acts synergistically, conferring high levels of resistance.

Using Transgenic Mosquitoes Overexpressing P450s to Assess Negative Cross Resistance to Proinsecticides. Initially we gathered published data on metabolic activity of CYP6P3 and CYP9K1, in the form of substrate depletion and formation of metabolites, toward the proinsecticides pirimiphos-methyl, indoxacarb, and chlorfenapyr (Table 3) (26, 31). As there were no data on the metabolism of indoxacarb by CYP6P3 and of pirimiphos-methyl by CYP9K1, we supplemented those by recombinantly expressing the two proteins and using them in metabolism assays. Both enzymes have been shown to metabolize chlorfenapyr to the active form tralopyril, while no other metabolite was detected by mass spectrometry with selected ion monitoring (31). Both enzymes also metabolize pirimiphos-methyl (here we show a 35% depletion of pirimiphos-methyl by CYP9K1, Table 3) and generate two metabolites: the active pirimiphos-methyl oxon and the oxidatively cleaved 2-diethylamino-6-hydroxyl-4-methylpyrimidine, with similar abundance (26) (*SI Appendix*, Fig. S8 *A–D*). Indoxacarb is also metabolized by both enzymes (here we show a 19.5% depletion by CYP6P3 and 60% by CYP9K1, Table 3). In the case of CYP6P3, a hydroxylated metabolite was identified. However, the exact place of the hydroxylation could not be determined and thus the metabolite remains uncharacterized (*SI Appendix*, Fig. S6 *A–D*). In the case of CYP9K1 both the active DCJW and a hydroxylated metabolite (again uncharacterized) were identified (*SI Appendix*, Fig. S7 *A–E*).

To test in vivo the balance between activation and detoxification of the proinsecticides, we used the Cyp9k1$^+$ and Cyp6p3$^+$ strains and exposed them to the proinsecticides through topical bioassays, which allow more precise insecticide doses to be administered. Both strains showed ~10-fold resistance to indoxacarb

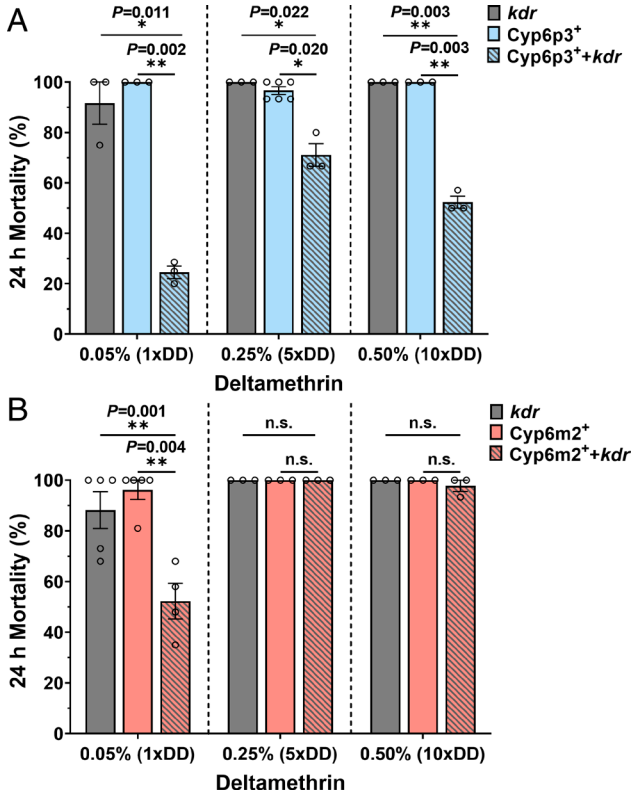

Fig. 5. Evaluating the combined effect of *Cyp6p3* or *Cyp6m2* overexpression with the VGSC mutation 995F (*kdr*) on pyrethroid resistance levels. (*A*) Percentage mortality of mosquitoes: overexpressing *Cyp6p3* (Cyp6p3$^+$), carrying the L995F mutation (*kdr*) or having the combination of the two mechanisms (Cyp6p3$^+$+*kdr*) 24 h after 1 h exposure to 1× (0.05%), 5× (0.25%) and 10× (0.50%) WHO diagnostic dose of deltamethrin. (*B*) Percentage mortality of mosquitoes: overexpressing *Cyp6m2* (Cyp6m2$^+$), carrying the L995F mutation (*kdr*) or having the combination of the two mechanisms (Cyp6m2$^+$+*kdr*) 24 h after 1 h exposure to 1× (0.05%), 5× (0.25%) and 10× (0.50%) WHO diagnostic dose of deltamethrin. For all bioassays, at least three replicates were performed, each comprising 12 to 25, 3 ~ 5-day-old females. Individual data points represent different biological replicates, and bars indicate the SE. Statistical significance was assessed using Welch's *t* test (n.s., not significant, **P* < 0.05, ***P* < 0.01; ****P* < 0.001).

(compared to the A11 control strain). Cyp6p3$^+$ was 1.9-fold more susceptible to chlorfenapyr and 1.7-fold to pirimiphos-methyl. Cyp9k1$^+$ was 2.5-fold more susceptible to chlorfenapyr and 2.4-fold to pirimiphos-methyl (Table 4). We also tested resistance levels to the proinsecticides when combining the overexpression of *Cyp6p3* and *Cyp9k1*. Overexpression of both genes (expression levels shown in *SI Appendix*, Fig. S2*E*) resulted in a small but significant change in the susceptibility to indoxacarb compared to Cyp9k1$^+$ and Cyp6p3$^+$ mosquitoes. No difference was observed in chlorfenapyr and pirimiphos methyl susceptibility by coexpression (Fig. 6).

Discussion

Mosquito population control tools that are based on insecticides have succeeded in preventing millions of malaria cases and deaths (2). However, the selection of high levels of insecticide resistance in *An. gambiae* populations, which is a result of the extensive use of these tools and our reliance on a few active ingredients (27), is now threatening their efficacy. Several studies have analyzed insecticide resistance in *An. gambiae* populations at a transcriptomic and genomic level, associating a plethora of genes and genomic alterations with the phenotype. However, very few of these genes and alterations, that are also frequently coexisting, have been functionally validated and it remains largely unknown what their effect size is.

We used the GAL4-UAS system to overexpress in susceptible *An. gambiae* mosquitoes the *Cyp9k1* P450 and the *Abch2* transporter. These two genes have been previously associated with resistance to pyrethroids, but without in vivo functional validation (12, 19, 32). *Cyp9k1* has been found overexpressed in several Anopheles resistant populations and the gene locus shows signals of positive selection (33, 34). In vitro metabolism assays have shown CYP9K1's ability to metabolize deltamethrin and the insect growth regulator pyriproxyfen (12). In this study, we show that its overexpression in multiple tissues, under the polyubiquitin promoter results (29) in resistance to all pyrethroids tested at the WHO diagnostic dose, with the highest resistance ratio against α-cypermethrin (30-fold). A smaller, but significant increase in tolerance to DDT was also observed, while no resistance was detected to the organophosphates malathion and pirimiphos-methyl and the carbamate bendiocarb. The pyrethroid resistance profile of *Cyp9k1* overexpressing mosquitoes is similar to those previously generated in *Cyp6p3* and *Cyp6m2* overexpressing mosquitoes (all three-show resistance to permethrin and deltamethrin), but differs in relation to nonpyrethroid insecticides (14). *Cyp6p3* and *Cyp6m2* overexpressing mosquitoes did not show resistance to DDT. Furthermore *Cyp6p3* mosquitoes, in contrast to *Cyp9k1*, did show resistance to bendiocarb. Thus, populations overexpressing both *Cyp6p3* and *Cyp9k1* could be multiresistant to pyrethroids, DDT, and bendiocarb.

We also functionally validated the role of the ABCH2 transporter. Transient silencing of the *Abch2* expression was previously shown to result in increased mortality upon deltamethrin exposure and increased penetration of the insecticide, as measured using radiolabeled insecticide (19). The gene was also found to be expressed in mosquitoes' appendages and specifically in the epithelial cells of the legs, underneath the cuticle. Here, we show that

Table 2. Time-response toxicity assays for estimating resistance strength in mosquitoes carrying combinations of target site and metabolic resistance

Line	Insecticides	LT_{50}	95% FL	Slope ± SE	RR
A10	Deltamethrin	2.99	1.93 – 4.06	3.11 ± 0.30	–
kdr	Deltamethrin	18.92	13.44 – 25.20	2.57 ± 0.24	6.33
Cyp6p3$^+$	Deltamethrin	11.35	8.50 – 13.98	2.56 ± 0.23	3.80
Cyp6m2$^+$	Deltamethrin	7.26	4.56 – 10.66	1.613 ± 0.15	2.48
Cyp6p3$^+$+*kdr*	Deltamethrin	174.63	129.95 – 305.53	2.23 ± 0.30	58.40
Cyp6m2$^+$+*kdr*	Deltamethrin	79.65	54.33 – 112.73	1.97 ± 0.19	26.63

Mosquitoes carrying the VGSC L995F mutation (*kdr*), overexpressing one of the two P450s (*Cyp6p3*, *Cyp6m2*), or having a combination of the two mechanisms (Cyp6p3$^+$+*kdr*, Cyp6m2$^+$+*kdr*) were exposed to the 1× WHO diagnostic dose of deltamethrin at varying exposure times. The LT_{50} (time in min required to obtain 50% mortality) is provided for each strain with the 95% fiducial limits (95% FL). The resistance ratio (RR) (LT_{50} of resistant strain/LT_{50} of control) is given in comparison with the A10 control strain. For each LT_{50}, a minimum of five exposure time points were tested with at least three replicates per time point. Each replicate includes 12 to 25, 3 ~ 5-day-old female mosquitoes.

Table 3. Metabolic activity of recombinantly expressed CYP6P3 and CYP9K1 for chlorfenapyr, Indoxacarb, and pirimiphos-methyl

Protein	Insecticides	Depletion	Identified metabolites	Note
CYP6P3	Indoxacarb	19.5%	• Hydroxylated (uncharacterized)	This study
	Chlorfenapyr	>80%	• Tralopyril (active)	(31)
	Pirimiphos-methyl	100%	• Pirimiphos methyl-oxon (active)	
			• Oxidatively cleaved: 2-diethylamino-6-hydroxyl-4-methylpyrimidine	(26)
CYP9K1	Indoxacarb	60%	• DCJW (active)	This study
			• Hydroxylated (uncharacterized)	
	Chlorfenapyr	>90%	• Tralopyril (active)	(31)
	Pirimiphos-methyl	35.9%	• Pirimiphos methyl-oxon (active)	This study
			• Oxidatively cleaved (2-diethylamino-6-hydroxyl-4-methylpyrimidine)	

Percentage depletion of each insecticide measured by HPLC and formation of metabolites detected with mass spectrometry.

overexpression of *Abch2* in multiple tissues (including the appendages), under the polyubiquitin promoter did not confer resistance to the WHO diagnostic dose of any insecticide tested (19). However, we observed a clear reduction in deltamethrin susceptibility (resistance ratio of approximately eightfold), when using a three times lower deltamethrin dose. Thus, the overexpression of *Abch2* alone most likely confers only a mild insensitivity and may not be a primary resistance mechanism. However, we need to note that the use of the polyubiquitin promoter might not fully mirror the internal expression pattern (tissue and cell specific) of the genes tested and the levels of overexpression achieved might not be equivalent to those in resistant populations. Although, for example, *Cyp6p3* and *Cyp9k1* have been reported to be overexpressed in field populations by approximately 4 to 12-fold, and *Abch2* to be induced 2.8-fold following deltamethrin exposure (12, 25, 35) direct comparison with expression levels achieved here using the GAL4/UAS system is not possible. This is because the GAL4/UAS system used drives broad expression across multiple tissues, which may not reflect the relative overexpression levels in the tissues relevant for detoxification. Thus, the actual levels of resistance conferred by a gene, could be over or under estimated. In the future the system would greatly benefit from the availability of different promoters including tissue and cell specific, as well as inducible ones.

Resistant mosquitoes often harbor multiple resistance mechanisms (12, 22–25). This can arise through coselection events, for example, when loci are physically close on the genome and belong to the same gene cluster exhibiting copy-number variation (36, 37), or when selection acts on a trans-regulator that alters the expression of several enzymes simultaneously (38–40). In such cases, functional redundancy may or may not be present. Multiple resistance mechanisms can also accumulate through sequential selection events. Here, selection pressure may come from exposure to different classes of insecticides, leading to the emergence of multiresistant phenotypes. An example is the overexpression of detoxification enzymes that metabolize distinct insecticide classes, such as GSTE2, which metabolizes DDT (14, 16), and CYP6P3, which metabolizes pyrethroids and bendiocarb (14, 26). Another driver for the accumulation of resistance mechanisms would be the selection for increased resistance strength.

Here we demonstrate a synergistic interaction between target-site and metabolic resistance mechanisms. The combination of the L995F mutation in the VGSC with the overexpression of either *Cyp6p3* or *Cyp6m2* produced greater than multiplicative resistance ($RR_{combined} > RR_{mechanism\ 1} \times RR_{mechanism\ 2}$). In the case of the Cyp6p3$^+$+*kdr* combination, we found significantly high resistance even to the 10× WHO diagnostic dose. This is in line with previous studies showing synergistic effects between target site and metabolic resistance mechanisms using *Drosophila* as a model organism (41) or in mosquitoes (10, 17, 42). In this study, we expand this observation and show that combined overexpression of two detoxification enzymes (in this case of *Cyp6p3* with either *Abch2*, *Cyp9k1*, *Coeae6g*, or *Gste2*) can also result in significantly higher resistance levels than those conferred by each enzyme individually. In some combinations, the effect was particularly pronounced, such as the *Cyp6p3* and *Cyp9k1* combination, where resistance was observed not only to the 1× diagnostic dose of permethrin and deltamethrin but also at the 5× diagnostic dose.

The mechanisms underlying these synergistic interactions remain poorly understood. For combinations of target-site mutations with

Table 4. Evaluating sensitivity to proinsecticides in Cyp6p3$^+$ and Cyp9k1$^+$ mosquitoes through dose response toxicity assays

Line	Insecticides	LD_{50} (ng/mosquitoes)	95% FL	Slope ± SE	RR
A11	Indoxacarb	1.12	0.69 – 1.58	1.42 ± 0.14	
	Chlorfenapyr	3.82	3.21 – 4.66	3.14 ± 0.38	
	Pirimiphos-methyl	1.71	1.34 – 2.22	2.61 ± 0.23	
Cyp6p3$^+$	Indoxacarb	12.49	10.27 – 15.14	1.76 ± 0.17	11.16
	Chlorfenapyr	2.05	1.80 – 2.34	2.82 ± 0.25	−1.86
	Pirimiphos-methyl	1.05	0.90 – 1.21	3.03 ± 0.26	−1.62
Cyp9k1$^+$	Indoxacarb	11.40	8.78 – 14.84	1.38 ± 0.19	10.20
	Chlorfenapyr	1.59	1.22 – 2.07	2.04 ± 0.24	−2.40
	Pirimiphos-methyl	0.74	0.63 – 0.85	2.56 ± 0.21	−2.31

Toxicity bioassays through topical application of insecticides were performed in mosquitoes overexpressing *Cyp6p3* and *Cyp9k1*, as well as control mosquitoes (A11). The LD_{50} (concentration causing 50% mortality) with 95% FL is provided for each strain. Resistance ratio (RR) is provided in comparison to A11 (LD_{50} of Cyp6p3$^+$/Cyp9k1$^+$ divided by LD_{50} of A11). For the estimation of LT_{50}, at least five concentrations were tested, each including at least three biological replicates. For each replicate, twenty 3 ~ 5-day-old female mosquitoes were tested.

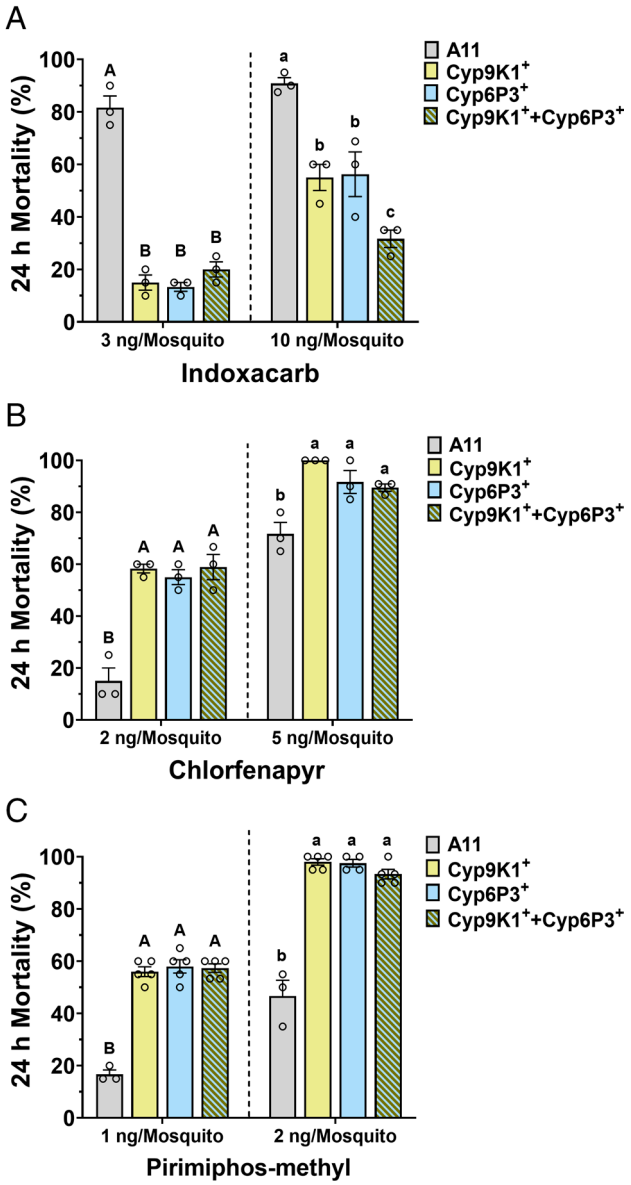

Fig. 6. Evaluating the effect of combined *Cyp6p3* and *Cyp9k1* overexpression on the susceptibility to proinsecticides. (*A*) Percentage mortality of mosquitoes overexpressing *Cyp9k1* (Cyp9k1$^+$), *Cyp6p3* (Cyp6p3$^+$), or their combination (Cyp9k1$^+$+Cyp6p3$^+$) 24 h after topical application of 3 and 10 ng of indoxacarb per mosquito, that are equivalent to the LD_{20} and LD_{50} of the Cyp6p3$^+$strain (*B*) 2 and 5 ng chlorfenapyr per mosquito, that are equivalent to the LD_{50} and LD_{90} of the Cyp6p3$^+$ strain, (*C*) 1 and 2 ng pirimiphos-methyl per mosquito, equivalent to the LD_{50} and LD_{90} of the Cyp6p3$^+$ strain. For all bioassays, at least three replicates were performed, each comprising twenty 3 ~ 5-day-old females. Individual data points represent different replicates, and bars indicate the SE. Statistical significance was assessed using one-way ANOVA followed by a Tukey's test.

overexpressed detoxification enzymes, one possibility is that the reduced binding affinity of the insecticide to the mutated VGSC allows more time for detoxification enzymes to metabolize the insecticide (if they are also overexpressed in the target tissues). Alternatively, detoxification enzymes may reduce the amount of insecticide that reaches the VGSCs in the target tissue, which combined with decreased binding affinity, results in a synergistic decrease in the channel's inhibition. Similarly, how different detoxification enzymes act synergistically is not yet experimentally proven. In our system, the combined effect of P450s is unlikely to result simply from higher total P450 levels. This is supported by two observations: First, Cyp6p3$^+$+Cyp6p3$^+$ mosquitoes, despite having higher *Cyp6p3* expression than either GAL4-Cyp6p3$^+$ or Cyp6p3$^+$ mosquitoes, were not more resistant, and second, Cyp6p3$^+$+Cyp9k1$^+$ mosquitoes were more resistant compared to Cyp6p3$^+$, despite having lower *Cyp6p3* expression and similar *Cyp9k1* expression. A plausible hypothesis on how different detoxification enzymes could act in combination is that they form assemblies with enhanced metabolic activity. Indeed, there are indications from research in mammals that P450s can interact and their complexes may have altered substrate turnover efficiency (43, 44). Alternatively, different detoxification enzymes may act sequentially in a metabolic cascade that enhances insecticide clearance (45). In such a scenario, the metabolite produced by one enzyme, which can retain toxicity, could serve as the substrate for another enzyme that may even exhibit higher affinity for the metabolite than for the parental compound (46). Sequential metabolism could also prevent the loss of catalytic efficiency that occurs when a single enzyme is required to process both the parental insecticide and its metabolites, which can compete for the active site (11). This mechanism has been proposed for CYP6M2, which metabolizes deltamethrin and has also been shown to further transform some of its initial metabolites (11). Furthermore, it has been shown that while CYP6Z2 (another P450 frequently overexpressed in pyrethroid resistant mosquitoes), cannot metabolize pyrethroids (the parental compounds), it metabolizes PBAlc and PBAld, the major metabolites produced by other pyrethroid metabolizing P450s (47).

We also showed that when the overexpression of *Abch2* is combined with the overexpression of a metabolic enzyme, in this case CYP6P3, it can increase the levels of resistance conferred by the P450. In this combination, the two mechanisms could act independently; the ABCH2 may export a portion of the insecticide not permitting its internalization, while CYP6P3 metabolizes the internalized molecules. Therefore, when combined they achieve a greater reduction in the number of active molecules reaching the nervous system.

We also assessed the susceptibility of Cyp6p3$^+$ and Cyp9k1$^+$ mosquitoes to the proinsecticides chlorfenapyr, pirimiphos-methyl, and indoxacarb. Mosquitoes overexpressing P450s are expected to be more vulnerable to proinsecticides that require P450 mediated activation. Both CYP6P3 and CYP9K1 have previously been shown to activate the mitochondrial blocker chlorfenapyr in vitro, by generating the metabolite tralopyril (31). Our in vivo data build on these in vitro findings, to show that when *Cyp6p3* and *Cyp9k1* are overexpressed in mosquitoes there is an increase in chlorphenapyr susceptibility relative to controls. An increase in susceptibility was also observed to pirimiphos-methyl, despite the production of an oxidatively cleaved metabolite alongside the active pirimiphos-methyl oxon in vitro. This suggests that in vivo the rate of pirimiphos methyl activation by these P450s exceeds the rate of its oxidative cleavage, at least when exposed by topical application. The relatively low increase in susceptibility we observed in Cyp6p3$^+$ and Cyp9k1$^+$ mosquitoes indicates that the endogenous P450 activity is likely sufficient to activate the proinsecticides and that additional P450 expression, at least in the tissues dictated by the ubiquitin promoter, does not alter the balance between activation and detoxification.

In contrast to pirimiphos methyl and chlorfenapyr, Cyp6p3$^+$, and Cyp9k1$^+$ mosquitoes exhibited approximately 10-fold resistance to indoxacarb. This was expected for CYP6P3 given that only a hydroxylated metabolite was identified in vitro. In the case of CYP9K1, where both a hydroxylated and the active DCJW were identified, the toxicity test implies that the generation of the less toxic hydroxylated metabolite is the predominant pathway in vivo. In contrast to the combined effect which we observed between *Cyp6p3* and *Cyp9k1* overexpression in conferring resistance to pyrethroids, only minor effects were observed for the balance of activation/

detoxification of the proinsecticides tested. This difference in indoxacarb metabolism indicates that the combined effect of different P450 coexpression is insecticide specific and may involve the action of the different detoxification enzymes at different sites of the insecticide molecule, which is in line with a sequential metabolism model.

The data presented in this study not only advance our understanding on the mechanisms of insecticide resistance and how these translate to phenotypic resistance, but also have important implications for the design of efficient insecticide resistance management strategies. The demonstrated combined effects of different resistance mechanisms underscore the need to revise both the design and interpretation of molecular diagnostics used in field populations. Currently all molecular diagnostics evaluate resistance markers (mutations, overexpression levels) independently and the interpretation of the results is restricted to the presence and frequency of resistant alleles (or overexpression rates of detox genes) (25, 48, 49). Our findings show, however, that the interaction among multiple mechanisms can ultimately shape resistance levels. This strongly supports the development of multiloci diagnostics capable of predicting not only the presence of resistance, but also its magnitude in field mosquito populations. Different combinations of resistance mechanisms are likely to produce varying outcomes, ranging from synergistic and additive to no or even antagonistic effects, and of different magnitude. Therefore, future studies should explore a broad range of combinations to define phenotypic outcomes and identify underlying patterns. Furthermore, our results highlight the importance of evaluating, in vivo, the presence of cross or negative-cross resistance to proinsecticides, mediated by the overexpression of P450s circulating in field populations. Such assessments must be conducted on a case-by-case basis to avoid failure of resistance-management strategies that rely on proinsecticide activation (in the case of cross resistance) and at the same time leverage the power of these compounds to combat highly pyrethroid resistant populations, in the case of negative cross resistance. Finally, this work has contributed important synergism data to the considerable progress made over the past decades in understanding insecticide resistance and developing evidence-based management strategies, however our knowledge of resistance is still incomplete. Further research is needed to fully elucidate the dynamics of the different mechanisms that underpin insecticide resistance particularly in field resistant populations, that better reflect natural conditions.

Materials and Methods

Mosquito Rearing. All mosquitoes were reared at 26 ± 2 °C and 70 ± 10% relative humidity under a 12:12 h light–dark photoperiod cycle. Larvae were fed ground fish food (Tetramin Tropical Flakes; Tetra, Blacksburg, VA, USA), and adults were maintained with 10% sucrose solution ad libitum.

Creation of UAS-Abch2 and UAS-Cyp9k1 Responder Lines. Generation of UAS-Abch2 and UAS-Cyp9k1 responder lines followed a previously described approach. Briefly, the coding sequence of *Abch2* (AGAP0003680, 2283 bp) and *Cyp9k1* (AGAP000818, 1596 bp) was amplified from the susceptible Kisumu strain using Phusion High-Fidelity DNA polymerase (New England Biolabs, Herts, UK) and primers listed in *SI Appendix*, Table S4. The coding sequence was subcloned into the pGEM-T Easy vector (Promega, Madison, USA) and then cloned into the pSL*attB:YFP:Gyp:UAS14i:Gyp:attB plasmid, downstream of the UAS as a NheI/XhoI (for *Abch2*) and EcoRI/NcoI (for *Cyp9k1*) restriction enzyme fragment. The structure of the responding plasmids is shown in *SI Appendix*, Fig. S1 *A* and *B*. Plasmids were sequenced to verify no differences in the cloned sequences compared to Vector base reference sequences.

To generate the responder lines, embryos from the A11 docking line, carrying a 3xP3-eCFP marker and two inverted attP sites, were injected with 150 ng/μL of the integrase helper plasmid pKC40 (encoding phiC31 integrase) mixed with 350 ng/μL of the responder plasmid, following previously described procedures (14, 29). Transient positive F_0 individuals (YFP signal in their anal papillae) were sexed prior to emergence, pooled into founder cages and outcrossed with wild-type G3 mosquitoes. To obtain homozygous responder lines virgin F_1 progeny carrying exclusively the YFP marker (indicative of cassette exchange) were crossed to males of the parental A11 docking line (labeled with CFP). F_2 progeny were intercrossed, and homozygous UAS-Abch2 and UAS-Cyp9k1 strains were established by selecting individuals carrying only the YFP marker. Details of embryo injections and the generation of the UAS-Abch2 and UAS-Cyp9k1 responder lines are provided in *SI Appendix*, Fig. S1 *A* and *B* and Table S2.

Creation of the Ubi-A10: UAS Cyp6p3 Line. Generation of a line that natively overexpresses *Cyp6p3* under the Ubiquitin promoter: the responder plasmid generated and used to make the UAS-Cyp6p3 line in Adolfi et al. (14) was injected in embryos of the Ubi-A10 driver line (14), carrying a 3× P3-eCFP marker and two inverted attP sites, using the same procedures described above. Transiently positive F_0 individuals were sexed as pupae and outcrossed with G3 mosquitoes. F_1 progeny carrying both YFP and CFP markers in the eyes and nerve cord (indicative of cassette integration) were retained and outcrossed with G3 to expand the strain for one generation, while wild-type individuals lacking fluorescence were removed each generation. Details of embryo injections and the generation of Ubi-A10: UAS Cyp6p3 driver line are provided in *SI Appendix*, Fig. S4*A* and Table S2.

Establishment of Ubi-GAL4+kdr, UAS-Cyp6p3+kdr, and UAS-Cyp6m2+kdr Lines. The Kisumu^{995F} (*kdr*) line generated and described in Grigoraki et al. (10) was crossed with the Ubi- GAL4 driver line (14) (CFP^+ marked) and the UAS-Cyp6p3 and UAS-Cyp6m2 responder lines (14) (YFP^+ marked), respectively. Progeny of the crosses (F_1) were backcrossed to the Kisumu^{995F} line to obtain F_2 homozygotes for the mutation. F_2 individuals were screened for the presence of the YFP^+ or CFP^+ markers. Individuals positive for the fluorescent signal were retained and left to emerge individually. The pupae case was used to extract DNA and select homozygotes for the *kdr* mutation using an LNA diagnostic assay, as previously described (10). Homozygotes of the *kdr* were intercrossed and thereafter kept as a mix of heterozygotes and homozygous for the GAL4 and UAS transgenic cassettes (Ubi-GAL4+*kdr*, UAS-Cyp6p3+*kdr*, and UAS-Cyp6m2+*kdr*) (*SI Appendix*, Fig. S5 *A–C*). Screening and selection of YFP^+ and CFP^+ positive individuals was performed each generation to enrich the frequency of the transgenic cassettes. To obtain individuals that over express the *Cyp6p3* or *Cyp6m2* and are homozygous for the *kdr* mutation, YFP^+ individuals from the UAS-Cyp6p3+*kdr* and UAS-Cyp6m2+*kdr* lines were crossed to CFP^+ individuals from the Ubi-GAL4+*kdr* line. Progenies that were both YFP and CFP positive were used in WHO susceptibility bioassays (*SI Appendix*, Fig. S5 *D* and *E*).

Relative Gene Expression Analysis. For gene expression analysis, total RNA was extracted from progeny of the different crosses using TRIzol reagent (Thermo Fisher Scientific, Waltham, USA) according to the manufacturer's instructions, with at least three biological replicates of six 3 ~ 5-day-old adults each. Genomic DNA was removed by treatment with RQ1 RNase-Free DNase (Promega). RNA concentration and purity were determined using a NanoDrop spectrophotometer, and first-strand cDNA was synthesized from 1 μg total RNA with the Engineered M-MLV Reverse Transcriptase Basic Kit (EnzyQuest, Heraklion, Greece) following the manufacturer's instructions. RT-qPCRs were set up by using KAPA SYBR FAST (Merck, Rahway, USA) kit, RT–qPCR was performed on a Bio-Rad CFX96 (Bio-Rad Laboratories, Hercules, USA), as previously described (19), with three biological replicates and two technical replicates per biological replicate. The relative expression of each gene was analyzed by using the Pfaffl (50) method with the *Ribosomal Protein S7* (AGAP010592) as reference gene (19). Graphs and statistical analyses were performed using GraphPad Prism version 8.2.1 (GraphPad Software; https://www.graphpad.com/), with Welch's *t* test and one-way ANOVA (Tukey's test) applied as appropriate.

Assessment of Insecticide Susceptibility.

WHO tube bioassays. To assess insecticide susceptibility in *An. gambiae*, WHO tube bioassays were conducted following standard protocols (30) using insecticide-impregnated papers (Vector Control Research Unit, University Sains Malaysia), including 0.05%, 0.25%, and 0.50% of deltamethrin, 0.75%, 3.75%, and 7.50% of permethrin, 0.05% of α-cypermethrin, 0.1% of bendiocarb, 4% of DDT, 5% of malathion, and 0.25% of pirimiphos-methyl, as previously described (10, 14). Different exposure times were used to estimate the LT_{50} of different insecticides, and PoLoPlus v2.0 (LeOra Software, Petaluma, USA) was used to

calculate the LT_{50} value, Resistance Ratio, and associated statistical parameters. For each time point, at least three replicates were performed, each consisting of approximately 20 females aged 3 to 5 day-old. The Knockdown rate was recorded immediately after the insecticide exposure and the mortality was recorded 24 h later. Welch's *t* test was used to evaluate statistical differences between mortality rates. Statistics were calculated using a GraphPad Prism version 8.2.1 (GraphPad Software; https://www.graphpad.com/).

Topical application bioassays. For topical application bioassays, indoxacarb (98.32%), chlorfenapyr (99.38%), and pirimiphos-methyl (97.00%) were purchased from Ehrenstorfer (LGC Labo, Augsburg, DE) and dissolved in acetone to prepare stock solutions at 10,000 mg L^{-1}. Working solutions of the desired concentrations were subsequently prepared by serial dilution with acetone. Female mosquitoes (3 to 5 d-old) were anesthetized on ice for 2 min, and 0.2 μL of each insecticide solution (and acetone control) was applied to the surface of the pronotum using a PB600-1 repeating dispenser (Hamilton Company, Reno, USA). For each dose, at least three replicates of 20 individuals each were tested. Mortality was assessed 24 h posttreatment, and bioassay data were analyzed using PoloPlus v2.0.

Functional Expression of Cytochrome P450s. Cytochrome P450 (P450) gene sequences were synthesized into the pCW-OmpA2 expression vector, while *Anopheles gambiae* cytochrome P450 reductase (*Ag*CPR) was cloned into pACYC, as described by Mclaughlin et al. (51). Coexpression of each P450 enzyme with *Ag*CPR was performed in *Escherichia coli* BL21 (DE3) Star cells. Membrane preparations were resuspended in 1× TSE buffer and stored at –80 °C. P450 content was quantified by CO-difference spectroscopy (52), and CPR activity was determined through NADPH-dependent cytochrome c reduction (53). Total protein concentration was measured using the Bradford assay (54).

To verify enzyme functionality, metabolism assays were conducted using permethrin and deltamethrin, which are known to be metabolized by CYP6P3 and CYP9K1 (20 μM), respectively (26). Each reaction (100 μL final volume) contained 20 pmol recombinant CYP, 200 pmol *An. gambiae* cytochrome b5 (AgCytb5) [Stevenson et al. (11)], 20 μM insecticide and an NADPH-generating system consisting of 1 mM glucose-6-phosphate, 0.1 mM NADP+, and 1 unit/mL glucose-6-phosphate dehydrogenase (G6PDH) in 0.2 M Tris–HCl buffer (pH 7.4) with 0.25 mM $MgCl_2$. Incubations were carried out at 30 °C and 1,250 rpm. Reactions were terminated by the addition of 100 μL acetonitrile, centrifuged at 13,000 rpm to remove precipitated proteins, and 100 μL from the resulting supernatants were analyzed by HPLC using a C18 reverse-phase column. Insecticides were eluted under isocratic conditions with water/acetonitrile mixtures (20:80 for permethrin and 10:90 for deltamethrin) at a flow rate of 1.25 mL/min for 20 min. Reactions were monitored by changes in absorbance between 225 to 250 nm and quantified by peak integration (Chromeleon, Dionex).

Cytochrome P450 Metabolism Assays for Indoxacarb and Pirimiphos-Methyl. Stock solutions of 10 mM indoxacarb (99.9% purity; Sigma-Aldrich, USA) and pirimiphos-methyl (99.9% purity; Sigma-Aldrich, USA) were prepared in acetonitrile.

(a) Indoxacarb and CYP6P3: Reactions of 100 μL contained 10 μM indoxacarb final organic solvent concentration of 1 % (v/v), 10 pmol CYP6P3 bacterial membrane protein, and 100 pmol AgCytb5 in 100 μL Tris–HCl buffer (0.2 M, pH 7.4) containing 0.25 mM $MgCl_2$.
(b) Pirimiphos-methyl and CYP9K1: Reactions of 100 μL contained 25 μM pirimiphos-methyl [final organic solvent concentration of 2.5 % (v/v)], 25 pmol CYP9K1 bacterial membrane protein, and 250 pmol AgCytb5 in 100 μL Tris–HCl buffer (0.2 M, pH 7.4) containing 0.25 mM $MgCl_2$.

Each incubation was performed in the presence and absence of an NADPH-generating system consisting of 1 mM glucose-6-phosphate, 0.1 mM $NADP^+$, and 1 unit/mL glucose-6-phosphate dehydrogenase (G6PDH; Sigma-Aldrich, USA). Reactions were incubated at 30 °C with 1,250 rpm oscillation and stopped at 0 h and 2 h time points by adding 100 μL acetonitrile. Samples were mixed and stirred for an additional 30 min to ensure complete quenching. The mixtures were centrifuged at 10,000 rpm for 10 min, and the resulting supernatants were transferred to LC vials. An aliquot of 10 μL of each supernatant was injected for LC–MS analysis using an Ultimate 3000 Autosampler (Thermo Scientific, USA). All reactions were performed in triplicates, and results were compared with negative control reactions without the NADPH-regenerating system to assess substrate depletion.

Identification of Indoxacarb and Pirimiphos-Methyl Metabolites by LC–MS Analysis. The reactions of CYP6P3 and CYP9K1 with indoxacarb and pirimiphos-methyl, respectively, in the presence and absence of an NADPH-generating system, were analyzed by LC-MS. Sample injections of 10 μL were performed using an Ultimate 3000 Autosampler (Thermo Scientific, USA). Chromatographic separation was achieved on an Ultimate 3000 system (Thermo Scientific, USA) equipped with a 3 μm C18 (100 × 2.1 mm) reverse-phase analytical column (Fortis Technologies, UK).

(a) Indoxacarb analysis: Indoxacarb reaction mixtures were analyzed with an isocratic mobile phase consisting of 70% acetonitrile and 30% H_2O, at a flow rate of 0.2 mL min^{-1} over a 10-min run. Detection was performed using an Electrospray Ionization (ESI) Q Exactive Hybrid Quadrupole-Orbitrap Mass Spectrometer (Thermo Scientific, USA) operated in positive ion mode. Mass spectrometric parameters were as follows: spray voltage 3,500 V, sheath gas pressure 20 arbitrary units., auxiliary gas pressure 25 arbitrary units, and ion-transfer capillary temperature 350 °C. Parallel Reaction Monitoring (PRM) of indoxacarb was performed using collision-induced dissociation (CID) at 10 to 20 eV, with high-purity nitrogen as the sheath, auxiliary, and collision gas.
(b) Pirimiphos-methyl analysis: Pirimiphos-methyl reaction mixtures were analyzed with an isocratic mobile phase consisting of 70% acetonitrile containing 0.1% formic acid and 30% H_2O containing 0.1% formic acid, at a flow rate of 0.3 mL min^{-1} over a 7-min run. Detection was carried out using the same ESI Q Exactive Hybrid Quadrupole-Orbitrap MS system in positive ion mode. Instrument parameters were spray voltage 4,000 V, sheath gas pressure 40 arbitrary units., auxiliary gas pressure 5 arbitrary units, and ion-transfer capillary temperature 300 °C. PRM was conducted using CID at 10 to 20 eV under high-purity nitrogen.

The instrument was operated in full-scan, extracted-ion monitoring (EIM), and parallel reaction monitoring (PRM) modes. Data acquisition and processing were carried out using Xcalibur software (v4.0, Thermo Scientific, USA).

Data, Materials, and Software Availability. Transgenic lines and plasmids described will be provided by L.G or G.J.L. on request. The raw bioassay data can be accessed at Figshare https://figshare.com/articles/dataset/Raw_data_of_Bioassay/32812793?file=65999243 (55). All other data are included in the manuscript and/or supporting information.

ACKNOWLEDGMENTS. We would like to thank Theodora Tatsiou for assisting with the generation of the UAS-Cyp9K1 plasmid used to generate the responder line and René Feyereisen for critically reviewing our manuscript. This publication is based on research funded by the Hellenic Foundation for Research and Innovation (H.F.R.I.) under the "3rd Call for H.F.R.I. Research Projects to support Post-Doctoral Researchers" (Project Number: 7406) (awarded to L.G.) and the call "Basic research Financing (Horizontal support of all Sciences)" under the National Recovery and Resilience Plan "Greece 2.0" funded by the European Union–NextGenerationEU (H.F.R.I. Project Number: 16044) (awarded to J.V.). M.C. acknowledges the support of the China Scholarship Council program (Project ID: 202306990018), L.R. is supported by a Marie Sklodowska-Curie Postdoctoral Fellowship, and J.M.F.O. and M.J.I.P. were funded by the IVCC (supported by the Bill and Melinda Gates Foundation under Grant Number OPP1148615) and the Medical Research Council (Grant Ref: MR/V001264/1).

Author affiliations: [a]Department of Biology, University of Crete, Heraklion 70013, Greece; [b]Institute of Molecular Biology and Biotechnology, Foundation for Research and Technology-Hellas, Heraklion 70013, Greece; [c]Vector Biology Department, Liverpool School of Tropical Medicine, Liverpool L3 5QA, United Kingdom; and [d]Department of Crop Science, Agricultural University of Athens, Athens 11855, Greece

Author contributions: M.J.I.P., G.J.L., J.V., and L.G. designed research; M.C., L.R., D.T., E.K., S.B., S.T., J.M.F.O., and L.G. performed research; G.J.L. contributed new reagents/analytic tools; M.C., L.R., D.T., E.K., J.M.F.O., M.J.I.P., and L.G. analyzed data; M.J.I.P., J.V., and L.G. secured funding; and M.C., J.H., J.V., and L.G. wrote the paper.

Reviewers: L.B., University of Wisconsin-Madison; L.L.K., University of the Witwatersrand; C.R., The University of Melbourne; and D.S., University of Florida.

1. WHO, WHO world malaria report 2025: Addressing the threat of antimalarial drug resistance. https://www.who.int/teams/global-malaria-programme/reports/world-malaria-report-2025.
2. S. Bhatt *et al.*, The effect of malaria control on Plasmodium falciparum in Africa between 2000 and 2015. *Nature* **526**, 207–211 (2015).
3. T. S. Churcher, N. Lissenden, J. T. Griffin, E. Worrall, H. Ranson, The impact of pyrethroid resistance on the efficacy and effectiveness of bednets for malaria control in Africa. *Elife* **5**, e16090 (2016).
4. H. Ranson, N. Lissenden, Insecticide resistance in African Anopheles mosquitoes: A worsening situation that needs urgent action to maintain malaria control. *Trends Parasitol.* **32**, 187–196 (2016).
5. V. A. Ingham, L. Grigoraki, H. Ranson, Pyrethroid resistance mechanisms in the major malaria vector species complex. *Entomol. Gen.* **43**, 515–526 (2023).
6. C. S. Clarkson *et al.*, The genetic architecture of target-site resistance to pyrethroid insecticides in the African malaria vectors *Anopheles gambiae* and *Anopheles coluzzii*. *Mol. Ecol.* **30**, 5303–5317 (2021).
7. V. A. Ingham, S. Wagstaff, H. Ranson, Transcriptomic meta-signatures identified in Anopheles gambiae populations reveal previously undetected insecticide resistance mechanisms. *Nat. Commun.* **9**, 5282 (2018).
8. R. Feyereisen, W. Dermauw, T. Van Leeuwen, Genotype to phenotype, the molecular and physiological dimensions of resistance in arthropods. *Pestic. Biochem. Physiol.* **121**, 61–77 (2015).
9. C. M. Jones *et al.*, Footprints of positive selection associated with a mutation (N1575Y) in the voltage-gated sodium channel of Anopheles gambiae. *Proc. Natl. Acad. Sci. U.S.A.* **109**, 6614–6619 (2012).
10. L. Grigoraki *et al.*, CRISPR/Cas9 modified An. gambiae carrying kdr mutation L1014F functionally validate its contribution in insecticide resistance and combined effect with metabolic enzymes. *PLoS Genet.* **17**, e1009556 (2021).
11. B. J. Stevenson *et al.*, Cytochrome P450 6M2 from the malaria vector Anopheles gambiae metabolizes pyrethroids: Sequential metabolism of deltamethrin revealed. *Insect Biochem. Mol. Biol.* **41**, 492–502 (2011).
12. J. Vontas *et al.*, Rapid selection of a pyrethroid metabolic enzyme CYP9K1 by operational malaria control activities. *Proc. Natl. Acad. Sci. U.S.A.* **115**, 4619–4624 (2018).
13. P. Muller *et al.*, Field-caught permethrin-resistant Anopheles gambiae overexpress CYP6P3, a P450 that metabolises pyrethroids. *PLoS Genet.* **4**, e1000286 (2008).
14. A. Adolfi *et al.*, Functional genetic validation of key genes conferring insecticide resistance in the major African malaria vector, Anopheles gambiae. *Proc. Natl. Acad. Sci. U.S.A.* **116**, 25764–25772 (2019).
15. N. Pavlidi, J. Vontas, T. Van Leeuwen, The role of glutathione S-transferases (GSTs) in insecticide resistance in crop pests and disease vectors. *Curr. Opin. Insect Sci.* **27**, 97–102 (2018).
16. J. M. Riveron *et al.*, A single mutation in the GSTe2 gene allows tracking of metabolically based insecticide resistance in a major malaria vector. *Genome Biol.* **15**, R27 (2014).
17. S. N. Mitchell *et al.*, Metabolic and target-site mechanisms combine to confer strong DDT resistance in Anopheles gambiae. *PLoS One* **9**, e92662 (2014).
18. S. Balaska *et al.*, Predictive chemoproteomics and functional validation reveal Coeae6g-mediated insecticide cross-resistance in the malaria vector Anopheles gambiae. *Nat. Commun.* **16**, 10772 (2025).
19. M. Kefi *et al.*, ABCH2 transporter mediates deltamethrin uptake and toxicity in the malaria vector Anopheles coluzzii. *PLoS Pathog.* **19**, e1011226 (2023).
20. L. Grigoraki *et al.*, Striking diflubenzuron resistance in Culex pipiens, the prime vector of West Nile Virus. *Sci. Rep.* **7**, 11699 (2017).
21. J. M. Riveron *et al.*, Directionally selected cytochrome P450 alleles are driving the spread of pyrethroid resistance in the major malaria vector Anopheles funestus. *Proc. Natl. Acad. Sci. U.S.A.* **110**, 252–257 (2013).
22. M. Bonizzoni *et al.*, RNA-seq analyses of changes in the *Anopheles gambiae* transcriptome associated with resistance to pyrethroids in Kenya: Identification of candidate-resistance genes and candidate-resistance SNPs. *Parasites Vectors* **8**, 474 (2015).
23. P. Muller, M. J. Donnelly, H. Ranson, Transcription profiling of a recently colonised pyrethroid resistant Anopheles gambiae strain from Ghana. *BMC Genomics* **8**, 36 (2007).
24. V. A. Ingham *et al.*, Integration of whole genome sequencing and transcriptomics reveals a complex picture of the reestablishment of insecticide resistance in the major malaria vector Anopheles coluzzii. *PLoS Genet.* **17**, e1009970 (2021).
25. J. Williams *et al.*, Characterisation of Anopheles strains used for laboratory screening of new vector control products. *Parasit Vectors* **12**, 522 (2019).
26. C. Yunta *et al.*, Cross-resistance profiles of malaria mosquito P450s associated with pyrethroid resistance against WHO insecticides. *Pestic. Biochem. Physiol.* **161**, 61–67 (2019).
27. WHO, Global insecticide use for vector-borne disease control A 10-year assessment. https://iris.who.int/server/api/core/bitstreams/de514069-9e2e-45f6-89fe-e00ac91a7d10/content.
28. H. Van den Berg *et al.*, Recent trends in global insecticide use for disease vector control and potential implications for resistance management. *Sci Rep* **11**, 23867 (2021).
29. A. Adolfi, E. Pondeville, A. Lynd, C. Bourgouin, G. J. Lycett, Multi-tissue GAL4-mediated gene expression in all Anopheles gambiae life stages using an endogenous polyubiquitin promoter. *Insect Biochem. Mol. Biol.* **96**, 1–9 (2018).
30. WHO, Standard operating procedure for testing insecticide susceptibility of adult mosquitoes in WHO bottle bioassays. https://www.who.int/publications/i/item/9789240043770.
31. C. Yunta *et al.*, Chlorfenapyr metabolism by mosquito P450s associated with pyrethroid resistance identifies potential activation markers. *Sci. Rep.* **13**, 14124 (2023).
32. C. S. Djoko Tagne *et al.*, A single mutation G454A in the P450 CYP9K1 drives pyrethroid resistance in the major malaria vector Anopheles funestus reducing bed net efficacy. *Genetics* **229**, 1–40 (2025).
33. S. C. Nagi, N. J. Harding, M. K. N. Lawniczak, M. J. Donnelly, A. Miles, An atlas of positive selection in the genomes of major malaria vectors. bioRxiv [Preprint] (2025). https://doi.org/10.1101/2025.07.16.664900 (Accessed 18 July 2025).
34. J. Hearn *et al.*, Multi-omics analysis identifies a CYP9K1 haplotype conferring pyrethroid resistance in the malaria vector Anopheles funestus in East Africa. *Mol. Ecol.* **31**, 3642–3657 (2022).
35. R. F. Djouaka *et al.*, Expression of the cytochrome P450s, CYP6P3 and CYP6M2 are significantly elevated in multiple pyrethroid resistant populations of *Anopheles gambiae* s.s. from southern Benin and Nigeria. *BMC Genomics* **9**, 538 (2008).
36. E. R. Lucas *et al.*, Copy number variants underlie major selective sweeps in insecticide resistance genes in Anopheles arabiensis. *PLoS Biol.* **22**, e3002898 (2024).
37. L. Grigoraki *et al.*, Carboxylesterase gene amplifications associated with insecticide resistance in Aedes albopictus: Geographical distribution and evolutionary origin. *PLoS Negl. Trop. Dis.* **11**, e0005533 (2017).
38. M. Ji *et al.*, A nuclear receptor HR96-related gene underlies large trans-driven differences in detoxification gene expression in a generalist herbivore. *Nat. Commun.* **14**, 4990 (2023).
39. L. B. Smith, R. Tyagi, S. Kasai, J. G. Scott, CYP-mediated permethrin resistance in Aedes aegypti and evidence for trans-regulation. *PLoS Negl. Trop. Dis.* **12**, e0006933 (2018).
40. R. Nauen, C. Bass, R. Feyereisen, J. Vontas, The role of cytochrome P450s in insect toxicology and resistance. *Annu. Rev. Entomol.* **67**, 105–124 (2022).
41. G. R. Samantsidis *et al.*, "What I cannot create, I do not understand": Functionally validated synergism of metabolic and target site insecticide resistance. *Proc. Biol. Sci.* **287**, 20200838 (2020).
42. M. C. Hardstone, C. A. Leichter, J. G. Scott, Multiplicative interaction between the two major mechanisms of permethrin resistance, kdr and cytochrome P450-monooxygenase detoxification, in mosquitoes. *J. Evol. Biol.* **22**, 416–423 (2009).
43. B. Dangi *et al.*, Probing functional interactions between cytochromes P450 with principal component analysis of substrate saturation profiles and targeted proteomics. *Arch. Biochem. Biophys.* **708**, 108937 (2021).
44. J. R. Reed, W. L. Backes, Formation of P450. P450 complexes and their effect on P450 function. *Pharmacol. Ther.* **133**, 299–310 (2012).
45. W. C. Black IV, T. K. Snell, K. Saavedra-Rodriguez, R. C. Kading, C. L. Campbell, From global to local-new insights into features of pyrethroid detoxification in vector mosquitoes. *Insects* **12**, 276 (2021).
46. Y. Gong, T. Li, Y. Feng, N. Liu, The function of two P450s, CYP9M10 and CYP6AA7, in the permethrin resistance of Culex quinquefasciatus. *Sci. Rep.* **7**, 587 (2017).
47. A. Chandor-Proust *et al.*, The central role of mosquito cytochrome P450 CYP6Zs in insecticide detoxification revealed by functional expression and structural modelling. *Biochem. J.* **455**, 75–85 (2013).
48. M. J. Donnelly, A. T. Isaacs, D. Weetman, Identification, validation, and application of molecular diagnostics for insecticide resistance in malaria vectors. *Trends Parasitol.* **32**, 197–206 (2016).
49. P. A. Hancock, E. Ochomo, L. A. Messenger, Genetic surveillance of insecticide resistance in African Anopheles populations to inform malaria vector control. *Trends Parasitol.* **40**, 604–618 (2024).
50. M. W. Pfaffl, A new mathematical model for relative quantification in real-time RT–PCR. *Nucleic Acids Res.* **29**, e45 (2001).
51. L. A. McLaughlin *et al.*, Characterization of inhibitors and substrates of Anopheles gambiae CYP6Z2. *Insect Mol. Biol.* **17**, 125–135 (2008).
52. T. Omura, R. Sato, The carbon monoxide-binding pigment of liver microsomes. *J. Biol. Chem.* **239**, 2370–2378 (1964).
53. H. W. Strobel, J. D. Dignam, Purification and properties of NADPH-Cytochrome P-450 reductase. *Methods Enzymol.* **52**, 89–96 (1978).
54. M. M. Bradford, A rapid and sensitive method for the quantitation of microgram quantities of protein utilizing the principle of protein-dye binding. *Analyt. Biochem.* **72**, 248–254 (1976).
55. M. Chen *et al.*, Data from "Synergistic action of different molecular mechanisms causes striking levels of insecticide resistance in the malaria vector *Anopheles gambiae*." Figshare. https://figshare.com/articles/dataset/Raw_data_of_Bioassay/32812793?file=65999243. Deposited 27 June 2026.